

ARTICLE

Received 10 Apr 2012 | Accepted 28 May 2012 | Published 26 Jun 2012

DOI: 10.1038/ncomms1926

Chloroplast-mediated activation of plant immune signalling in *Arabidopsis*

Hironari Nomura^{1,2}, Teiko Komori¹, Shuhei Uemura¹, Yui Kanda¹, Koji Shimotani¹, Kana Nakai¹, Takuya Furuichi³, Kohsuke Takebayashi⁴, Takanori Sugimoto⁴, Satoshi Sano¹, I Nengah Suwastika¹, Eiichiro Fukusaki⁴, Hirofumi Yoshioka^{2,5}, Yoichi Nakahira¹ & Takashi Shiina¹

Chloroplasts have a critical role in plant immunity as a site for the production for salicylic acid and jasmonic acid, important mediators of plant immunity. However, the molecular link between chloroplasts and the cytoplasmic-nuclear immune system remains largely unknown. Here we show that pathogen-associated molecular pattern (PAMP) signals are quickly relayed to chloroplasts and evoke specific Ca^{2+} signatures in the stroma. We further demonstrate that a chloroplast-localized protein, named calcium-sensing receptor (CAS), is involved in stromal Ca^{2+} transients and responsible for both PAMP-induced basal resistance and *R* gene-mediated hypersensitive cell death. CAS acts upstream of salicylic acid accumulation. Transcriptome analysis demonstrates that CAS is involved in PAMP-induced expression of defence genes and suppression of chloroplast gene expression possibly through $^1\text{O}_2$ -mediated retrograde signalling, allowing chloroplast-mediated transcriptional reprogramming during plant immune responses. The present study reveals a previously unknown chloroplast-mediated signalling pathway linking chloroplasts to cytoplasmic-nuclear immune responses.

¹ Graduate School of Life and Environmental Sciences, Kyoto Prefectural University, Sakyo-ku, Kyoto 606-8522, Japan. ² Graduate School of Bioagricultural Sciences, Nagoya University, Chikusa-ku, Nagoya 464-8601, Japan. ³ EcoTopia Science Institute, Nagoya University, Chikusa-ku, Nagoya 464-8603, Japan. ⁴ Graduate School of Engineering, Osaka University, Suita, Osaka 565-0871, Japan. ⁵ The Venture Business Laboratory, Ehime University, Bunkyo-cho, Matsuyama 790-8577, Japan. Correspondence and requests for materials should be addressed to T.S. (email: shiina@kpu.ac.jp).

Plants are continuously exposed to a variety of biotic and abiotic stresses, and have evolved an intricate network of signal transduction pathways leading to transcriptome and metabolic reprogramming. Pathogen-associated molecular patterns (PAMPs) are recognized by pattern-recognition receptors in the plasma membrane and activate an array of basal defence responses (PAMP-triggered immunity, PTI), whereas pathogen-derived effector proteins trigger hypersensitive response (HR) cell death at the site of pathogen infection and confine the spread of pathogens (effector-triggered immunity, ETI)¹. Plant immunity activates two parallel signal transduction pathways: cytoplasmic mitogen-activated protein kinase (MAPK) and Ca²⁺ signalling pathways leading to transcriptional reprogramming, and a chloroplast-mediated pathway leading to the generation of chloroplast-derived reactive oxygen species (ROS) and the production of defence-related hormones, such as salicylic acid (SA) and jasmonic acid (JA)². Possible involvement of chloroplasts in plant innate immunity has been discussed³. However, the molecular link between the chloroplast and cytoplasmic-nuclear immune signalling pathways remains largely unknown. In particular, it is not clear how immune signals are relayed to chloroplasts and how chloroplasts control the expression of nuclear-encoded defence genes.

Extracellular stimuli evoke Ca²⁺ signals in not only the cytoplasm, but also organelles such as mitochondria, peroxisomes and nuclei^{4,5}. For example, the massive accumulation of Ca²⁺ in mitochondria leads to the dysfunction of mitochondria and induction

of apoptosis of mammalian cells⁶. However, very few studies have focused on Ca²⁺ signals in chloroplasts. Calcium-sensing receptor (CAS)⁷ is a thylakoid membrane-associated Ca²⁺-binding protein involved in the regulation of cytoplasmic Ca²⁺ oscillations and extracellular Ca²⁺-induced stomatal closure^{8–10}.

Here we show that PAMP signals evoke a CAS-dependent transient Ca²⁺ signal in chloroplasts, and that CAS is involved in transcriptional reprogramming through ¹O₂-mediated retrograde signalling during plant innate immunity. This study is an important advancement in the understanding of cross talk between chloroplasts and the plant immune system.

Results

Biotic and abiotic stress-induced chloroplast Ca²⁺ signals. To measure the free Ca²⁺ concentration in the stroma, the calcium-sensitive bioluminescent protein aequorin was targeted to the chloroplast stroma using an ribulose-1,5-bisphosphate carboxylase (RBCS) signal peptide (Supplementary Fig. S1). As reported previously, stromal Ca²⁺ was maintained at a very low concentration, as low as that in the cytoplasm (Fig. 1a–f), suggesting that Ca²⁺ in chloroplasts is sequestered in the thylakoid lumen or by Ca²⁺-binding proteins¹¹. We found that the bacterial PAMP flagellin peptide (flg22) induces a rapid Ca²⁺ transient in the cytoplasm, followed by a long-lasting increase in the stromal free Ca²⁺ level (Fig. 1a). A similar stromal Ca²⁺ transient was also induced by the fungal PAMP chitin (Fig. 1b). On the other hand, control peptides

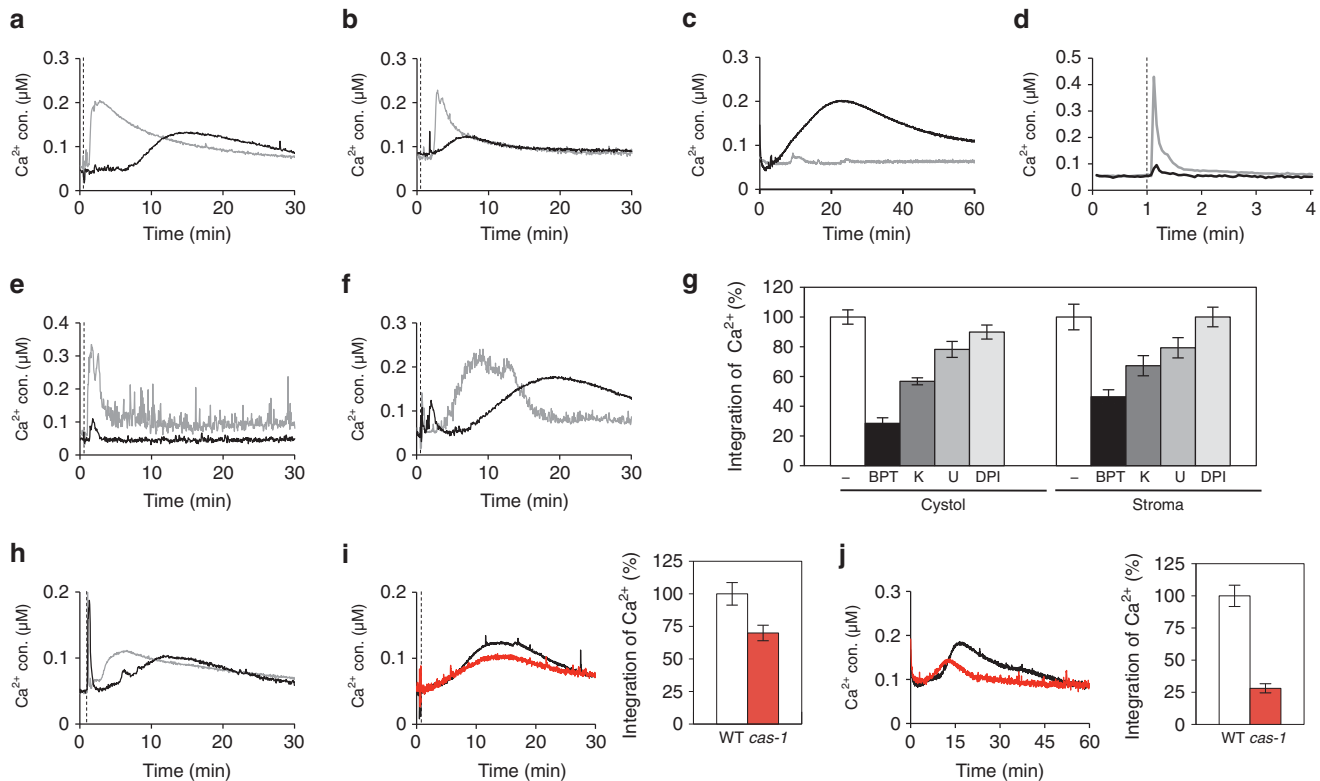


Figure 1 | Chloroplast Ca²⁺ dynamics. (a–f,h) Aequorin (AEQ) luminescence from wild-type (WT) AEQ-expressing plants treated with (a) 1 µM flg22, (b) 100 µg ml⁻¹ chitin, (c) light-to-dark transition, (d) ice-cold MS medium, (e) 200 mM NaCl, (f) 500 mM sorbitol or (h) 30 µM ionomycin. The vertical dashed line indicates the time at which treatment was initiated. Experiments were repeated at least five times, with control treatments. Representative data are shown. Cytosolic and stromal Ca²⁺ changes are indicated by grey and black lines, respectively. (g) Effects of signal transduction inhibitors on flg22-induced cytosolic and stromal Ca²⁺ increase in WT AEQ-expressing plants. ‘-’: no inhibitor, BPT: 5 mM 1,2-bis(2-aminophenoxy)ethane *N,N,N,N*-tetraacetic acid (BAPTA), K: 2 µM K252a, U: 20 µM U-0126, DPI: 50 µM DPI. The time-integrated cytosolic or stromal Ca²⁺ concentration upon 30-min treatment with 1 µM flg22 is shown. Data are the means ± s.e.m. of relative values (*n* = 4, control values were set of 100%). (i,j) Stromal Ca²⁺ changes in WT (black lines, white bars) and *cas-1* knockout (red lines and bars) plants expressing AEQ. Plants were treated with (i) 1 µM flg22 or (j) light-to-dark transition. The integrated stromal Ca²⁺ concentration was reduced in *cas-1* compared with WT. Data are the means ± s.e.m. of relative values (*n* = 4).

induced no Ca^{2+} signal in chloroplasts (Supplementary Fig. S2a). Furthermore, a *flg22*-induced stromal Ca^{2+} transient was observed in transplastomic tobacco plants in which the aequorin gene had been integrated into the chloroplast genome (Supplementary Fig. S2b), confirming the occurrence of Ca^{2+} dynamics in the chloroplast stroma. These findings demonstrate that extracellular PAMP signals are relayed rapidly to chloroplasts and evoke intrachloroplastic Ca^{2+} transients.

We further examined the effects of abiotic stresses on cytoplasmic and stromal Ca^{2+} signals. Light-to-dark transition evoked a slow Ca^{2+} transient in the stroma, but not the cytoplasm (Fig. 1c)¹¹. We also found that other abiotic stresses induced stromal Ca^{2+} transients in a stress-dependent manner. Cold and salt stresses elicited rapid stromal Ca^{2+} spikes within a minute, whereas hyperosmotic stress induced a biphasic long-lasting Ca^{2+} transient in the stroma (Fig. 1d–f). Stress-specific Ca^{2+} signatures in the stroma may be involved in the regulation of photosynthesis and metabolic processes in response to the given stresses.

In mammals, signal molecules such as staurosporine initially stimulate an increase in the cytoplasmic Ca^{2+} concentration, and subsequently induce a mitochondrial Ca^{2+} increase before apoptosis⁶. Similarly, PAMP-induced stromal Ca^{2+} transients were always preceded by cytoplasmic Ca^{2+} changes. We found that both chloroplastic and cytoplasmic Ca^{2+} changes were markedly decreased by the extracellular Ca^{2+} chelator 1,2-bis(2-aminophenoxy)ethane *N,N,N',N'*-tetraacetic acid (BAPTA; Fig. 1g). Furthermore, the Ca^{2+} ionophore ionomycin induced a biphasic Ca^{2+} increase in both the cytoplasm and the stroma (Fig. 1h). Interestingly, the second ionomycin-induced stromal Ca^{2+} increase was preceded by the cytoplasmic Ca^{2+} transient. From these results, we presume that PAMPs first induce Ca^{2+} entry into the cytoplasm and, subsequently, the cytoplasmic Ca^{2+} triggers a transient increase in the stromal Ca^{2+} concentration. In addition, both the cytoplasmic and stromal Ca^{2+} oscillations were partially reduced by inhibitors of serine/threonine protein kinase (K252a) and MAPKKs (U-0126), but not by an NADPH oxidase inhibitor (DPI; Fig. 1g), suggesting the possible involvement of a MAP kinase cascade in the generation of cytoplasmic and stromal Ca^{2+} signals.

CAS is involved in chloroplast Ca^{2+} signals. CAS is a plant-specific thylakoid-associated Ca^{2+} -binding protein^{8–10,12}. To examine the possible role of CAS in the generation of stromal Ca^{2+} transients, we measured *flg22*-induced stromal Ca^{2+} transients in aequorin-expressing plants with a CAS knockout background (*cas-1*). The aequorin-expressing *cas-1* plants accumulated the same amount of aequorin protein as wild-type plants (Supplementary Fig. S1a). We found that *flg22*- and dark-induced long-lasting stromal Ca^{2+} transients were markedly reduced in *cas-1* (Fig. 1i,j), whereas cold-induced rapid stromal Ca^{2+} spikes were not impaired in *cas-1* (Supplementary Fig. S3). Considering the localization of CAS in thylakoid membranes, CAS may be involved in Ca^{2+} release from thylakoid membranes and the generation of a long-lasting stromal Ca^{2+} signal.

CAS is responsible for both PTI and ETI. The presence of PAMP-induced Ca^{2+} transients in the stroma underscores the importance of chloroplasts in plant immune signalling. We found that *cas-1* plants exhibited severely impaired resistance to the virulent bacterium *Pseudomonas syringae* pv. *tomato* (*Pst*) strain DC3000 and to avirulent *Pst* DC3000 varieties (Fig. 2a). Surprisingly, PAMP (*flg22*)-induced defence-related events, such as stomatal closure (Fig. 2b), callose deposition (Fig. 2c) and accumulation of defence-related phenylpropanoids/flavonoids and their precursors (Supplementary Fig. S4), were markedly compromised in *cas-1*. Furthermore, *flg22*-induced *PR1* and *PR2* expression and stomatal closure were suppressed in two independent homozygous T-DNA insertion lines, *cas-1* and *cas-2* (ref. 8), whereas expression of CAS cDNA at wild-type levels in *cas-1* restored *flg22*-induced *PR1* and *PR2* expression

and stomatal closure (Fig. 2d, Supplementary Fig. S5). These results demonstrate that the chloroplast protein CAS is involved in a range of basal defence responses. We further found that *flg22*-induced stomatal closure was impaired by the NADPH oxidase inhibitor diphenyleneiodonium (DPI) and by the nitric oxide (NO) scavenger 2-(4-carboxyphenyl)-4,4,5,5-tetramethylimidazole-1-oxyl-3-oxide (cPTIO) in wild-type plants (Fig. 2e). On the other hand, exogenous application of hydrogen peroxide (H_2O_2) or the NO donor sodium nitroprusside (SNP) could induce stomatal closure in *cas-1* (Fig. 2f), suggesting that CAS acts upstream of ROS and NO signals in *flg22*-induced stomatal closure.

Some pathogens secrete effector proteins (*Avr* gene products) that suppress PTI. Conversely, effectors are recognized by plant proteins, which activate ETI leading to hypersensitive cell death at the infection site. We found that the *cas-1* plants exhibited delayed and suppressed HR cell death compared with the wild type after inoculation with *Pst* DC3000 (*avrRpt2*; Fig. 3a,b). Interestingly, the *Pst* DC3000 (*avrRpt2*)-induced accumulation of ROS (Supplementary Fig. S6a,b) and NO (Supplementary Fig. S6c,d) was significantly reduced in *cas-1* plants. Functional proof that CAS is a critical component in plant cell death was further demonstrated using virus-induced gene silencing (VIGS) in *Nicotiana benthamiana* plants. We cloned *NbCAS* from *N. benthamiana* (Supplementary Fig. S7a) and used VIGS to reduce its expression to <1% of the wild-type level (Supplementary Fig. S7b). *NbCAS* silencing resulted in a clear delay in the elicitor protein INF1-, the *cf9/Avr9* elicitor/receptor- and the constitutively active *N. tabacum* MAP kinase kinase (NtMEK2^{DD})-dependent cell death (Fig. 3c,d, Supplementary Fig. S7c), suggesting that CAS has a conserved role in plant cell death and may act downstream of the MAP kinase cascade in ETI. Considering a chloroplast localization of CAS, the above results suggest that chloroplasts might have critical roles in the positive regulation of plant immunity.

CAS regulates SA biosynthesis. It is unlikely that the compromised immunity of CAS knockout plants is caused by limited cellular resources, as *cas-1* plants are photosynthetically competent⁸ and do not show severe growth retardation (Supplementary Fig. S8). Chloroplasts are involved in the biosynthesis of plant hormones such as SA, JA, abscisic acid (ABA), indole-3-acetic acid (IAA) and cytokinins (CKs). Thus, we examined the profiles of a set of plant hormones (SA, JA, ABA, IAA and CKs) during *flg22*-induced PTI. The accumulation of free SA was transiently induced by *flg22* treatment within 6 h in wild-type plants, whereas JA and other hormones showed no significant change in levels (Fig. 4a–e), confirming a crucial role of SA in PTI signalling. Importantly, we found that CAS deficiency prevented *flg22*-induced accumulation of free SA (Fig. 4a) as well as glycosylated SA (Supplementary Fig. S9). As the basal SA levels before *flg22* treatment were normal in *cas-1* plants, CAS is likely involved in the regulation of SA biosynthesis rather than the biosynthesis itself. SA is synthesized in chloroplasts via the chorismate pathway in *Arabidopsis*¹³. It has been shown that PAMPs induce SA biosynthesis in an ICS1-dependent manner^{14,15}. Interestingly, the *flg22*-induced early expression of *PAD4*, *EDS5*, *PBS3* and *ICS1*, all of which are essential for SA biosynthesis, was significantly reduced in *cas-1* plants before SA accumulation (~1 h; Fig. 4f). On the other hand, *PR1* expression was induced significantly by SA in *cas-1* plants similarly to in wild-type plants (Supplementary Fig. S10), indicating that the signal transduction pathways downstream of SA are independent of CAS. These results demonstrate that CAS is involved in *flg22*-induced SA biosynthesis through promoting the expression of nuclear-encoded SA biosynthesis genes.

CAS-dependent induction of nuclear-encoded defence genes. These findings led us to hypothesize that CAS may be involved in chloroplast-to-nucleus retrograde signalling to control the expression of nuclear-encoded defence genes, including SA biosynthesis

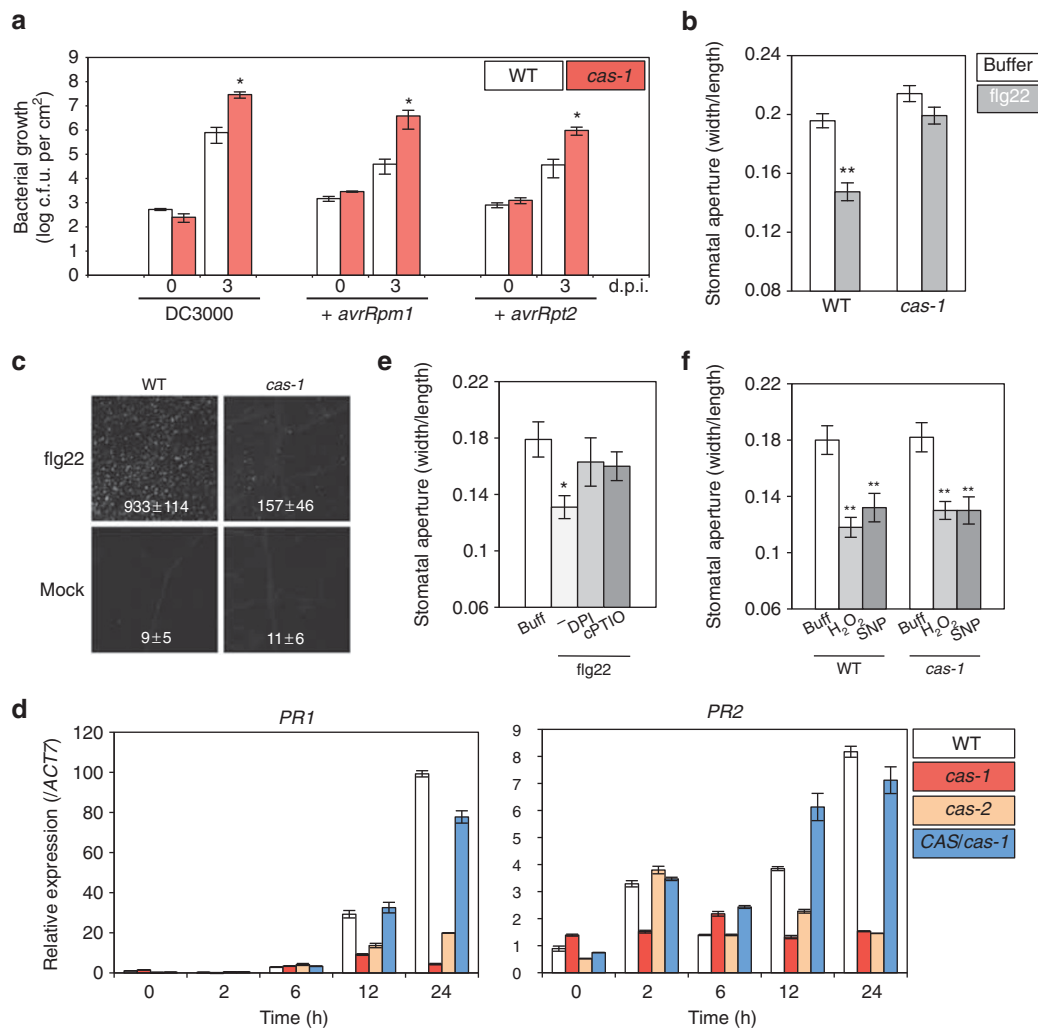


Figure 2 | Defects of immune regulation in *cas-1* mutants. (a) Bacterial growth of *Pseudomonas syringae* pv. *tomato* (*Pst*) in *Arabidopsis* leaves. Wild-type (WT) or *cas-1* plants were inoculated with virulent or avirulent *Pst* DC3000 ($OD_{600} = 0.0001$), and numbers of bacteria per leaf area on days 0 and 3 were plotted on a log scale. Data are the means \pm s.e.m. of relative values ($n = 4$; $*P < 0.05$, Student's *t*-test). The experiment was repeated three times, with similar results; d.p.i., days post infection. (b) Flg22-induced stomatal closure. The stomatal aperture was calculated as the ratio of the pore width/guard cell length. Data are the means \pm s.e.m. of 50 stomata from three replicates ($**P < 0.01$, Tukey-Kramer HSD test). (c) Detection of flg22-induced callose deposition with aniline blue. Representative pictures and the average number (with SD) of callose deposits per 4.5 mm^2 ($n = 8$) are shown. The experiment was repeated three times, with similar results. (d) Flg22-induced gene expression was analysed by qRT-PCR at the indicated time points. *ACT7* was used as an internal standard. Data are means \pm s.e.m. of relative values ($n = 3$). (e) Flg22-induced stomatal closure was inhibited in the presence of DPI or cPTIO. Leaves were pre-incubated with buffer (Buff) containing DPI or cPTIO for 30 min and then treated with $5 \mu\text{M}$ flg22 for 2 h. (f) Exogenously applied H_2O_2 and SNP could induce stomatal closure in *cas-1*. The stomatal aperture was calculated as the ratio of pore width/guard cell length. Data are the means \pm s.e.m. of 50 stomata (e: $*P < 0.05$, f: $**P < 0.01$, Tukey-Kramer HSD test).

genes. Flg22 induces the expression of numerous defence-related genes in the nucleus^{15,16}. To identify flg22-induced genes that are under the control of CAS, an *Arabidopsis* gene expression microarray (v4) was used to compare the flg22-induced transcription profiles of wild-type and *cas-1* plants. We identified 687 upregulated and 1,235 downregulated genes in *cas-1* plants treated with flg22 for 2 h (Fig. 5a and Supplementary Data 1 and 2). By contrast, only 7 genes were upregulated and 197 genes were downregulated in non-treated *cas-1* plants (Fig. 5a and Supplementary Data 3 and 4). In all, 121 of the 197 downregulated and 6 of the 7 upregulated genes in non-treated *cas-1* plants were also down- and upregulated in flg22-treated *cas-1* plants, respectively. Quantitative reverse transcription-PCR (qRT-PCR) confirmed the array results for selected targets (Figs 4f and 5c). Interestingly, the expressions of one-third (827 genes) of the flg22-induced early genes (within 3 h)¹⁷ were

suppressed in *cas-1* (Fig. 5a,b, Supplementary Fig. S11). Similarly, two-thirds of genes downregulated in flg22-treated *cas-1* were flg22-induced in wild type. Furthermore, the 403 genes upregulated in flg22-treated *cas-1* were enriched for genes that were suppressed by flg22 in wild type (58.7%). Gene expression analysis using the Expression Browser at Bio-Array Resource (BAR)¹⁸ showed that genes downregulated in flg22-treated *cas-1* were also enriched in NPP1- and HrpZ-responsive genes, as well flg22-responsive genes (Supplementary Fig. S12a). CAS, therefore, likely has a universal role in PAMP-induced gene expression.

Gene ontology analysis using the Arabidopsis Classification Super Viewer demonstrated a significant over-representation of 'response to stress' (3.04-fold, $P = 5.33\text{E} - 50$), 'response to abiotic and biotic stimulus' (2.49-fold, $P = 2.83\text{E} - 28$) and signal transduction (2.26-fold, $P = 7.17\text{E} - 14$) categories among the flg22-treated

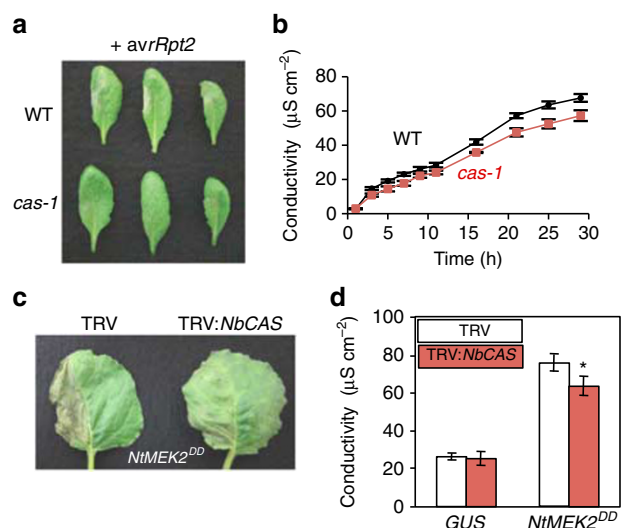


Figure 3 | CAS-dependent hypersensitive response (HR) cell death.

(a,b) HR after inoculation with avirulent *Pseudomonas syringae* pv. *tomato* (Pst) DC3000 (*avrRpt2*) (OD₆₀₀ = 0.05). (a) HR lesions on the left side of leaves at 14 h. (b) Ion leakage after inoculation was measured at the indicated time points in leaves of wild-type (WT; black line) and *cas-1* knockout (red line) plants. Data are the means ± s.e.m. of six discs from three replicates. (c) *NbCAS*-silenced *N. benthamiana* plants display a delay of cell death. Four- to five-week-old *NbCAS*-silenced plants were infiltrated with *Agrobacterium* containing the *NtMEK2^{DD}* expression vector. Tobacco rattle virus (TRV) was used as an experimental control. Pictures are taken at 3 days after inoculation. (d) Ion leakage at 3 days after infiltration with *Agrobacterium* containing *GUS* or *NtMEK2^{DD}* was measured in silenced leaves. Data are the means ± s.e.m. of six discs from three replicates. Significance was determined using Student's *t*-test (**P* < 0.05).

cas-1 downregulated genes (Supplementary Fig. S12b–e). The downregulated genes included a number of GTPase, Ca²⁺ signalling and SA signalling genes (Supplementary Data 5). CAS was also required for flg22-induced expression of *CYP79B2*, *CYP79B3* and *PAD3* genes for cytochrome P450 that are essential for the production of camalexin, the characteristic phytoalexin of *Arabidopsis*. On the other hand, the flg22-treated *cas-1* upregulated genes were enriched for those involved in 'electron transport or energy pathways' (2.34-fold, *P* = 1.34e-3). Interestingly, genes for plastid (1.93-fold, *P* = 1.46e-5) and chloroplast (1.86-fold, *P* = 5.29e-12) proteins were significantly enriched among the upregulated genes in flg22-treated *cas-1*. These results suggest that chloroplasts may promote defence gene expression and suppressing chloroplast (photosynthesis) gene expression through CAS during PTI.

Chloroplast regulation of nuclear transcriptional programmes.

We identified 99 and 78 transcription factor (TF) genes among the downregulated and upregulated genes in *cas-1*, respectively. WRKYs are a large family of plant-specific TFs (with 72 genes in *Arabidopsis*) that act mainly in the defence response network of plant cells^{19,20}. We identified one-third of WRKY genes under the control of CAS (25 downregulated and 1 upregulated; Supplementary Data 1), suggesting an important role for WRKYs in CAS-dependent PTI. In fact, the most represented motif in the promoters (500-bp upstream regions) of the flg22-treated *cas-1* downregulated genes was TTGAC (Supplementary Table S1). TTGAC is part of the W-box consensus sequence (TTGAC[C/T]) of the WRKY-binding site¹⁹. The W-box motif was found in the promoters of 539 of the 1,235 genes downregulated in flg22-treated *cas-1* (44%). The W-box sequences were enriched in the promoter region at 200–400 bp upstream of the translation start site (Supplementary Fig. S13), confirming the

W-box as a *cis*-element of the flg22-treated *cas-1* downregulated (CAS-dependent) genes. The flg22-treated *cas-1* downregulated TFs included several key factors, such as WRKY33 relaying the MAPK signal to the transcription network in PTI¹⁹, and WRKY28/WRKY46 (ref. 21) and CBP60g/SARD1 (ref. 22), essential for the activation of ICS1 and SA synthesis. Taken together, WRKY TFs might have a critical role in PAMP (flg22)-induced chloroplast-mediated transcriptional reprogramming in plant innate immunity.

By contrast, the upregulated TF genes included *AtGLK2* (ref. 23), *CIA2* (ref. 24), *GATA21*(*GNC*)²⁵ and a set of chloroplast sigma factors (*AtSIG1*, *AtSIG3*, *AtSIG4* and *AtSIG6*), which are required for chloroplast development²⁶. Interestingly, the I-box motif involved in light-responsive photosynthetic gene expression²⁷ was found in the promoters of 149 of the 687 genes upregulated in flg22-treated *cas-1* plants. Thus, it seems that chloroplasts (CAS) regulate plant immune responses through activation of defence-related TFs and suppression of chloroplast function/development by inactivating TFs required for chloroplast development.

Chloroplast-derived ROS and CAS-dependent gene expression.

To examine the role of flg22-induced TFs during early PTI, we performed a time course expression analysis using qRT-PCR. PAMP (flg22) triggered a rapid (within 15 min) and transient increase in the expression of TF genes such as *CBP60g*, *WRKY28*, *WRKY33* and *MYB122* (Fig. 5c), suggesting a role for them in early transcriptional reprogramming during PTI. On the other hand, the expression of *WRKY75* (Fig. 5c) and SA biosynthesis-related genes (Fig. 4f) peaked at 1–2 h, and *PR1* gene expression was induced after 12 h. Interestingly, flg22-induced early expression of TF genes (within 30 min) was not suppressed in *cas-1* mutants, but CAS was needed for the middle phase (1–2 h) expression of TF (Fig. 5c) and SA biosynthesis-related genes (Fig. 4f), and *PR1* gene expression at the late phase (24 h). On the other hand, overexpression of CAS hastened and enhanced early expression of a set of TF genes such as *CBP60g*, *WRKY33* and *MYB122* (Fig. 5c), suggesting a possible activating role of CAS in defence-related TF gene expression. These results imply that after a ~30-min lag chloroplasts may generate CAS-dependent retrograde signals, which is required for prolonged expression of the early defence-related TFs and promotes subsequent expression of defence-related genes. It has been proposed that chloroplast-derived ROS signals, such as ¹O₂ and H₂O₂, may activate the expression of nuclear-encoded defence genes^{28,29}. Notably, we found that 427 of 1,235 genes downregulated in flg22-treated *cas-1* overlapped with genes that were ¹O₂-responsive in the *flu* mutant (fold change > 3.0), including several ¹O₂ marker genes, *EDS5* and *ERD1* (Fig. 5b and Supplementary Data 1)²⁹. By contrast, only 153 genes overlapped with methyl viologen (MV)-induced O₂⁻/H₂O₂-responsive genes (fold change > 3.0; Supplementary Data 1)³⁰. These results suggest a role for CAS in ¹O₂ signalling to control nuclear-encoded defence gene expression.

Discussion

CAS is a plant-specific low-affinity/high-capacity non-EF-hand Ca²⁺-binding protein that is associated with thylakoid membranes of chloroplasts (Supplementary Fig. S14)^{8–10,12}. This study demonstrates that the chloroplast protein CAS is required for both PTI and *R* gene-mediated ETI. PTI and ETI are controlled by complex interconnected signalling networks including the MAP kinase cascade, ROS signalling and the plant hormones SA, JA and ethylene^{1,2}. We found that CAS may act upstream of ROS signalling in PAMP-induced stomatal closure, and downstream of the MAP kinase cascade and upstream of ROS/NO in ETI (Figs 2f, 3c and Supplementary Fig. S6). Furthermore, we demonstrated that CAS is required for the flg22-induced accumulation of SA (Fig. 4). Considering the chloroplast localization of CAS, these findings suggest that chloroplasts have a critical role in both PTI and ETI. CAS may

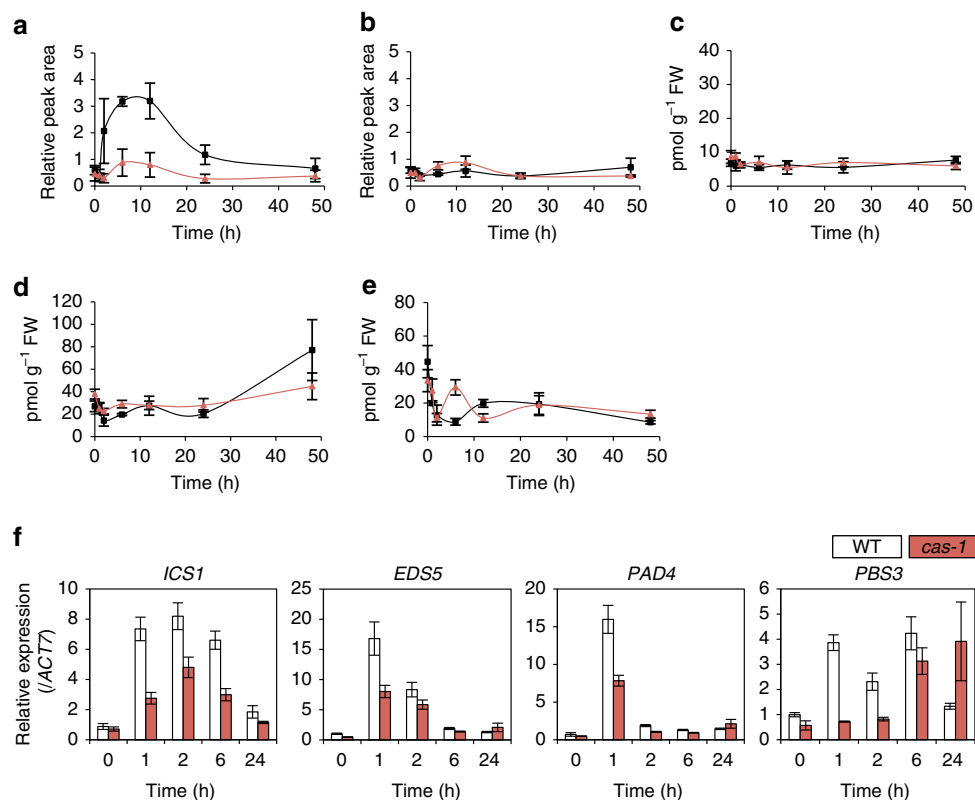


Figure 4 | CAS regulates salicylic acid (SA) biosynthesis and its related gene expression. (a–e) Flg22-induced phytohormone accumulation was measured at the indicated time points in leaves of wild-type (black line) and *cas-1* knockout (red line) plants. Data are the means \pm s.e.m. of three experiments. (a) SA and (b) jasmonic acid (JA) accumulation were measured using UPLC/TOFMS, and (c) abscisic acid (ABA), (d) indole-3-acetic acid (IAA) and (e) cytokinins were measured using nano-LC/MS/MS, and has been shown as the amount of hormones per fresh weight (FW) of plants. (f) Flg22-induced gene expression was analysed at indicated time points by qRT-PCR. *ACT7* was used as an internal standard. Data are mean \pm s.e.m. of three experiments.

be involved in the coupling of chloroplasts and cellular immune responses and may function upstream of ROS signalling and SA biosynthesis.

We found that CAS is required for transcriptional activation of SA biosynthesis genes, such as *ICS1*, *EDS5*, *PBS3* and *PAD4*, whereas the SA signalling pathway downstream of SA is not impaired in *cas-1* plants (Fig. 4 and Supplementary Fig. S10). Furthermore, microarray analysis revealed that the expression of a set of TF genes (*WRKY28/WRKY46* and *CBP60g/SARD1*)^{21,22}, essential for activation of SA biosynthesis genes, was greatly reduced in *cas-1* plants (Supplementary Data 1). These results suggest that CAS mediates the chloroplast control of SA biosynthesis through these TFs, and the resultant SA subsequently induces a range of basal defence responses. On the other hand, considering the co-localization of CAS and SA biosynthesis in chloroplasts, there remains a possibility that CAS might directly modulate *ICS1* activity within chloroplasts.

Recognition of pathogens results in a massive reprogramming of plant cells to activate defence responses and reduce other cellular activities, such as cellular development/organization and photosynthesis³¹. Microarray analysis demonstrates that CAS controls transcriptional reprogramming during PTI through activation of defence-related TFs including a number of WRKYs and suppression of TFs involved in chloroplast development. We found that a short DNA motif, W-box (TTGAC[T/C]), is over-represented in the promoter sequences of flg22-treated *cas-1* downregulated (CAS-dependent flg22-induced) genes (52.6%). The WRKY family TFs regulate biotic and abiotic stress responses and share the WRKY domain that recognizes the W-box¹⁹. Interestingly, the W-box is

over-represented not only in the promoter regions of defence-related genes, but also in O₃-responsive³² and superoxide-responsive promoters³⁰. On the other hand, some promoters of CAS-dependent flg22-suppressed genes contain an I-box motif, a common *cis*-element characteristic of photosynthesis genes (Supplementary Table S1)²⁷. Thus, these results suggest that CAS-dependent defence gene expression might be mediated by WRKY TFs that target W-box-containing promoters of plant defence genes in a ROS-dependent manner, whereas CAS may control PAMP-induced suppression of photosynthesis gene expression via an I-box-binding protein/I-box-mediated transcription system. Interestingly, some TF genes occur more rapidly in CAS-overexpressing plants, suggesting a direct role for CAS in the promotion of defence-related TF gene expression. However, the molecular function of CAS remains largely unknown. CAS deficiency may disrupt unidentified chloroplast function related to defence responses and indirectly affect the expression pattern of flg22-induced defence genes. Nevertheless, these findings strongly suggest that chloroplasts have a critical role in the transcriptional regulation of plant immune signalling.

It has been proposed that chloroplast-derived retrograde signals, such as chlorophyll synthesis intermediates and chloroplast-derived ROS, control the expression of nuclear-encoded genes for photosynthesis and defence responses³³, respectively. When the cell is unable to dissipate excess excitation energy, chloroplasts generate ROS, such as singlet oxygen (¹O₂) or hydrogen peroxide (H₂O₂), which activate distinct sets of genes. Interestingly, ¹O₂ triggers a cell death programme that resembles the effector-triggered HR³⁴. Here, we found that almost one-third of CAS-dependent flg22-induced genes are also induced by ¹O₂ in the *flu* mutant (Fig. 5b), but not by

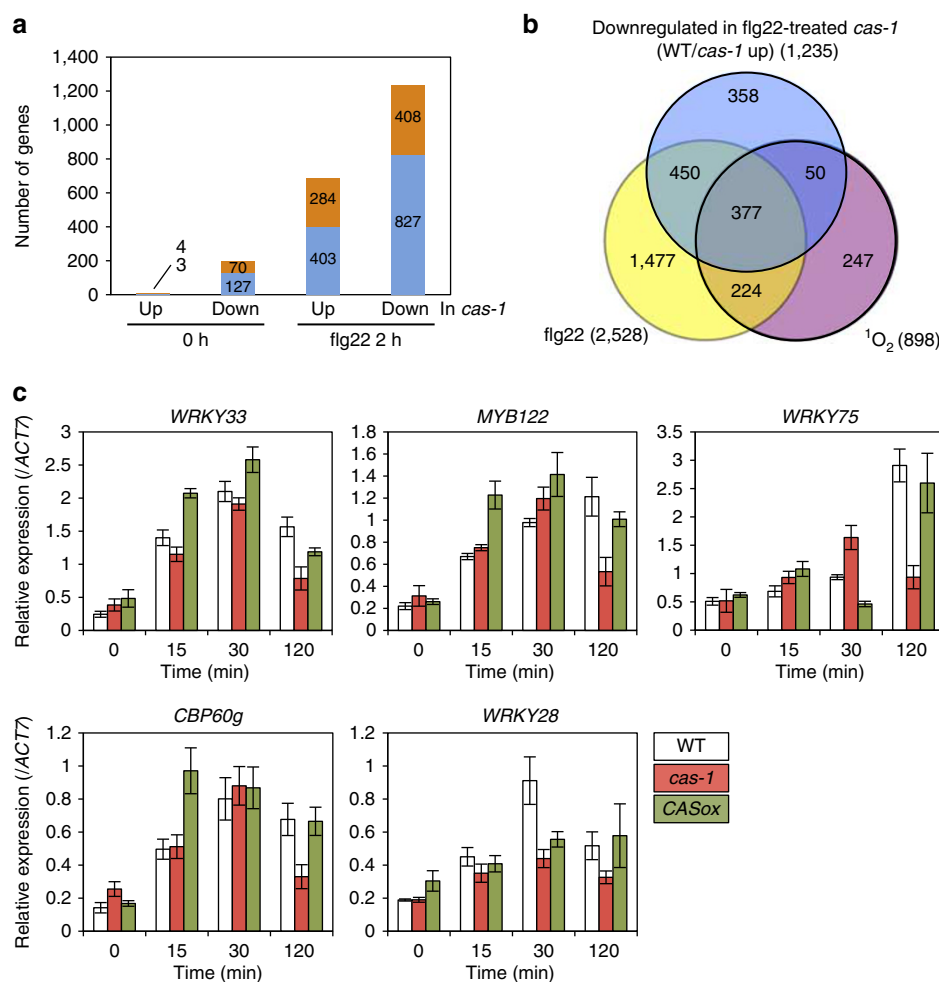


Figure 5 | Genome-wide transcriptional analysis of *cas-1* mutants in flg22-induced immunity. (a) Numbers of differentially expressed genes that were up- or downregulated in *cas-1* plants treated with flg22 for 2 h (right) or not treated (left). Genes that were regulated by flg22 within 3 h are shown in blue. Several flg22-induced genes were downregulated before flg22 treatment in *cas-1* plants. (b) Venn diagram showing the overlap of downregulated genes in flg22-treated *cas-1* (WT/*cas-1* up: blue), flg22-induced genes within 3 h (flg22: yellow) and chloroplastic $^1\text{O}_2$ -dependent genes under light for 2 h in the *flu* mutant background ($^1\text{O}_2$: purple). (c) Expression of flg22-induced genes was analysed at indicated time points by qRT-PCR to confirm microarray experiments. *ACT7* was used as an internal standard. Data are mean \pm s.e.m. of three experiments. WT, wild type.

MV-induced H_2O_2 . Furthermore, CAS-dependent flg22-induced genes also overlap with the light-induced genes in *flu* mutants overexpressing thylakoid-localized ascorbate peroxidase, which is expected to compensate for chloroplast-derived O_2^- and H_2O_2 , but not $^1\text{O}_2$ (ref. 29). These results suggest a role for chloroplast-derived $^1\text{O}_2$ signalling in CAS-dependent transcriptional control of nuclear-encoded defence genes. Moreover, the flg22-induced extracellular ROS burst was not impaired in *cas-1* plants (Supplementary Fig. S15), suggesting a limited role of NADPH oxidase-derived O_2^- and H_2O_2 in CAS-dependent immune responses. In addition, it has been recently shown by another group that extracellular Ca^{2+} -induced generation of chloroplast NO and ROS is dependent on CAS, but not plasma membrane-localized NADPH oxidase³⁵, providing further confirmation of the role of CAS in ROS production in chloroplasts. Thus, we assume that CAS may be involved in the chloroplast-derived $^1\text{O}_2$ -mediated retrograde signalling that regulates the expression of nuclear-encoded defence-related genes at an early stage in PTI. In fact, the release of $^1\text{O}_2$ in the *flu* mutant triggers the expression of *WRKY33* and *WRKY46* TFs during the first 30 min of reillumination³⁶, a subsequent drastic increase in free SA levels, and the expression of *PR1* and *PR5* genes³⁷. Time course qRT-PCR analysis revealed that chloroplasts generate signal(s) after a 30-min

lag time. Interestingly, it has been reported that Cle elicitor induces $^1\text{O}_2$ in cultured cells after a 10-min lag period, and peaks at 30 min after the treatment³⁸. This time course coincides well with those of flg22-induced defence-related gene expression and subsequent SA biosynthesis. We propose that a CAS-dependent chloroplast-derived signal (possibly $^1\text{O}_2$) may modulate the defence responses through transcriptional reprogramming of defence-related genes.

Therefore, it is speculated that pathogen signals are transmitted to chloroplasts before the production of chloroplast-derived ROS signal(s). Sai and Johnson¹¹ previously reported that light-to-dark transition triggers a transient rise of stromal free Ca^{2+} levels in tobacco chloroplasts. Here, we show that PAMPs evoke a long-lasting stromal Ca^{2+} increase following a rapid cytoplasmic Ca^{2+} transient (Fig. 1a,b). It is known that the thylakoid lumen accumulates Ca^{2+} at a high level. CAS is responsible for the full activation of long-lasting stromal Ca^{2+} transients induced by flg22 and darkness (Fig. 1i,j). Thus, it is plausible that CAS regulates the release and/or uptake of Ca^{2+} through thylakoid membranes to evoke long-lasting stromal Ca^{2+} signals. We further demonstrate that several abiotic stresses also induce stress-specific stromal Ca^{2+} signals (Fig. 1d-f), suggesting that stromal Ca^{2+} signatures may be involved in stress-specific responses, including rapid inhibition of photosynthesis and

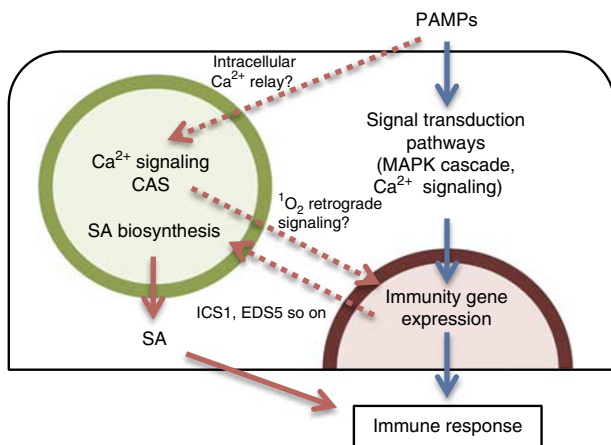


Figure 6 | Molecular cross talk between chloroplasts and cytoplasmic-nuclear immune system. Pathogen-associated molecular pattern (PAMP) signals are quickly relayed to chloroplasts and evoke specific Ca^{2+} signatures in the stroma. The thylakoid-associated calcium sensor protein CAS is involved in the generation of chloroplast Ca^{2+} signals. CAS is also essential for the induction of PAMP-induced defence genes, including salicylic acid (SA) biosynthesis genes, possibly through singlet oxygen ($^1\text{O}_2$)-mediated retrograde signalling. Thus, SA-mediated immune responses are dependent on CAS. Chloroplast-mediated pathways involved in the communication between chloroplasts and the cytoplasmic-nuclear signal transduction pathways are shown as dotted red arrows. The cytoplasmic and SA-mediated immune pathways are shown as red and blue arrows, respectively.

accumulation of JA^{39,40}. Interestingly, chloroplasts contain several EF-hand Ca^{2+} sensor proteins and other types of Ca^{2+} -binding proteins⁴¹.

PAMP-induced stromal Ca^{2+} transients precede CAS-dependent defence gene expression and SA biosynthesis, suggesting a role for chloroplast Ca^{2+} signatures in the activation of defence gene expression. Interestingly, genes induced by some abiotic stimuli such as light-to-dark transition and osmotic stress, which evoke long-lasting stromal Ca^{2+} signals, were enriched among genes downregulated in flg22-treated *cas-1*, but cold and salt-induced genes were not (Supplementary Fig. S16). The W-box sequences were also over-represented in the promoter regions of genes upregulated by osmotic stress, but not of cold and salt stimuli-induced genes (Supplementary Tables S1 and S2). Thus, chloroplast Ca^{2+} signatures are likely involved in stress-specific gene expression. It has been shown that Ca^{2+} regulates FBpase^{42,43}, and the stability of the photosystem II and thylakoid O_2 evolving complexes⁴⁴. The stromal Ca^{2+} transients coincide with the stress-induced rapid downregulation of photosynthesis^{39,45,46}. Importantly, photosynthesis collapse may lead to photo-induced production of ROS including $^1\text{O}_2$ (ref. 47). Taken together, long-lasting stromal Ca^{2+} signals may induce the down-regulation of photosynthetic electron flow, leading to the production of ROS. Interestingly, *cas-1* mutants show higher values of non-photochemical chlorophyll fluorescence quenching than do wild-type plants⁸. Non-photochemical chlorophyll fluorescence quenching has a major role in the protection of the photosynthetic apparatus against damage by excess light and the production of ROS⁴⁸.

Herein, we demonstrated a novel chloroplast-dependent pathway that controls plant innate immunity through stromal Ca^{2+} signalling and chloroplast-to-nuclei retrograde ROS signalling (Fig. 6). Recent studies have shown that plant innate immune responses are modified by light and intrinsic circadian cues^{49,50}. Chloroplasts may act as an environmental sensor in plants⁵¹. Interestingly, CAS is required for photoacclimation in *Chlamydomonas*¹².

Furthermore, CAS has been shown to be involved in the coupling of diurnal extracellular Ca^{2+} oscillations to cytosolic Ca^{2+} oscillations⁵². Characterization of the molecular function of CAS and chloroplast Ca^{2+} signalling would provide insight into the role of chloroplasts in cross talk among environmental regulation pathways and plant immunity.

Methods

Plant materials and growth conditions. *Arabidopsis thaliana* wild-type Columbia ecotype, CAS knockout mutants (*cas-1* and *cas-2*)⁸, CAS-overexpressing plants⁸ and apoaquorin transgenic plants were germinated and grown on one-half Murashige and Skoog (MS) medium containing 0.8% (w/v) agar at 22°C with 16-h light (80–100 $\mu\text{mol m}^{-2} \text{s}^{-1}$)/8-h dark cycles for 2–4 weeks. For pathogen inoculation experiments, 4- to 5-week-old wild-type and *cas-1* plants grown on soil with 10-h light (140–160 $\mu\text{mol m}^{-2} \text{s}^{-1}$)/14-h dark cycles were used.

Measurements of cytosolic and stromal Ca^{2+} concentrations. Ca^{2+} measurements were performed as previously described, with some modifications⁸. Detached rosette leaves from plate-grown transgenic wild-type and *cas-1* *Arabidopsis* plants expressing aequorin were floated on one-half MS liquid medium containing 5 μM coelenterazine, then kept overnight at 22°C in the dark. Aequorin luminescence was measured with Lumi Counter 2500 (Microtec). The amount of reconstituted aequorin in the plants was determined by the addition of an equal volume of 2 M CaCl_2 in 20% ethanol at the end of the measurements. Aequorin luminescence calibration was performed as previously described⁵³.

Elicitor peptide flg22 was synthesized by Biologica (Nagoya). The chitin suspension was prepared as previously described⁵⁴. Chitin (Wako) was hydrolysed with concentrated HCl, and left for 2 h at room temperature with occasional mixing. The hydrolysed chitin was then washed with water twice, and dissolved in one-half MS medium to achieve a final chitin concentration of 1.0 mg ml^{-1} . Cold shock stress was applied to the plants by adding ice-cold one-half MS medium to a leaf floated in a cuvette. The measurement of dark-stimulated Ca^{2+} changes was performed as described¹¹. Ten-day-old plants were incubated at 22°C under 24-h light conditions (22 $\mu\text{mol m}^{-2} \text{s}^{-1}$), and then transferred to the dark. In pharmacological experiments, BAPTA (Wako), K-252a (Wako), U-0126 (Calbiochem) or DPI (Calbiochem) were dissolved in ethanol or DMSO and applied to plants in a cuvette at the appropriate concentration and left for 30 min before treatment with flg22.

Plant inoculation and quantification of bacteria. Pathogen inoculations, bacterial growth counts and ion conductance measurements were performed as previously described, with some modifications⁵⁵. The virulent strain of *Pst* DC3000 and avirulent strains of *Pst* DC3000 (carrying *avrRpt2* or *avrRpm1*) were cultured at 28°C in King's B medium containing 25 $\mu\text{g ml}^{-1}$ kanamycin, 100 $\mu\text{g ml}^{-1}$ rifampicin and 50 $\mu\text{g ml}^{-1}$ cycloheximide, washed once in 10 mM MgCl_2 and resuspended in 10 mM MgCl_2 . Needleless syringe infiltration was used to inoculate plants with pathogen in all cases. Immediately after the infiltration, the plants were allowed to dry and were then kept under 100% humidity for the remainder of the experiment. At indicated time points, leaf discs were collected, ground to homogeneity in water and the titre was determined by serial dilution and plating.

For measurements of ion leakage, 6 leaf discs (8-mm diameter) were removed immediately following infiltration ($t=0$) and floated in 25 ml of water. After 30 min, the water was removed and replaced with 10 ml of new water. The conductance of this water was measured at the indicated time points.

Stomatal aperture measurements. Stomatal aperture measurements were performed as previously described⁸. Rosette leaves from 3- to 4-week-old plate-grown plants were detached and floated on the incubation buffer (10 mM 2-(N-morpholino)ethanesulfonic acid (MES)-KOH, pH 6.15; 10 mM KCl; 50 μM CaCl_2) for 2 h at 22°C, in 80–100 $\mu\text{mol m}^{-2} \text{s}^{-1}$ light. After 2 h, the leaves in the incubation buffer were treated with or without 5 μM flg22, 10 μM H_2O_2 or 50 μM SNP and then incubated for an additional 2 h. For inhibitor experiments, the leaves were pre-incubated with 50 μM DPI or 200 μM cPTIO for 30 min before treatment with flg22. After the incubation period, epidermal strips of the leaves were observed by microscopy. The stomatal aperture was calculated as the ratio of the pore width/guard cell length. A guard cell length of 22–28 μm was used in the experiments.

Callose deposition. Rosette leaves of 4- to 5-week-old soil grown wild-type and *cas-1* plants were infiltrated with 10 mM Tris-HCl (pH 7.2; mock) or the same solution containing 5 μM flg22. After 24 h, the leaves were detached, cleared with ethanol and stained with 10 mM Tris-HCl (pH 7.2) containing 0.01% aniline blue for 30 min. Leaves were stored in 50% glycerol and observed via epifluorescence microscopy under UV illumination with a broadband DAPI filter set. Measurements of callose deposition were made using the image-processing software IMAGEJ.

Metabolite analysis by nano-LC/MS/MS and UPLC/TOFMS. Levels of SA, JA, ABA, IAA, zeatin and zeatin riboside were analysed by nano-liquid chromatography – tandem mass spectrometry (LC/MS/MS) with a modification

of the methods described by Izumi *et al.*⁵⁶. Briefly, 100 mg of leaf samples were homogenized using a ballmill and extracted with methanol/H₂O/formic acid (75:20:5) solution containing internal standards (40 pmol (d₇-DHZOG, d₃-DHZR, d₆-iP, d₆-iPR), 200 pmol (d₆-ABA), 400 pmol (d₃-DHZ), 1,000 pmol (d₂-GA₁, d₅-IAA, d₂-GA₇), 2 μmol lidocaine and 10 μmol (+)-10-camphorsulfonic acid). After centrifugation, half of the supernatant was used for analyses of SA, JA and small charged molecules by ultra-performance liquid chromatography – time-of-flight mass spectrometry (UPLC/TOFMS) as described previously^{56,57}. The remaining supernatant was extracted with water and dried. The dried samples were dissolved in 1 M formic acid and applied to the OASIS MCX cartridge. The fraction containing ABA and IAA was eluted with methanol and, subsequently, the CK fraction was eluted with 60% methanol solution containing 0.35 M NH₄. Eluted fractions were further purified and analysed by nano-LC/MS/MS.

SA was also measured using a conventional high-performance liquid chromatography system. A total of 200 mg of seedling samples without roots was homogenized and extracted with 100% methanol containing the internal standard anisic acid. Free and glycosylated SA were separated and analysed by high-performance liquid chromatography.

VIGS and Agrobacterium-mediated transient expression. VIGS was done as described by Ratcliff *et al.*⁵⁸. pBINTRA6 (RNA1) and the pTV00 containing the *NbCAS* cDNA fragment (RNA2) were transformed by electroporation separately into *Agrobacterium tumefaciens* strain GV3101 (pSoup). A mixture of equal parts of *Agrobacterium* suspensions of RNA1 and RNA2 was infiltrated into 2- to 3-week-old *N. benthamiana* leaves.

For cell death assay, *Agrobacterium* strain GV3101 (pSoup) carrying *NtMEK2^{DD}*, *INP1*, *cf9/Avr9* or *GUS* (pGreen binary vectors) was infiltrated into the upper leaves of 4- to 5-week-old *NbCAS*-silenced *N. benthamiana* plants.

Microarray experiments and data analysis. The genome-wide microarray analyses were performed using the *Arabidopsis* v4 2 colour microarray (Agilent Technologies). Light grown, 2-week-old, wild-type and *cas-1* mutant plants were floated on one-half MS medium for 1 day (0 h), and then treated with 1 μM flg22 for 2 h. Total RNA was isolated with the Qiagen RNeasy plant mini kit following the manufacturer's instructions. Two independent biological replicates were performed for each sample and control. Each 200-ng total RNA sample was used to prepare Cy3- or Cy5-labelled target cRNA with the Low Input Quick Amp Labelling Kit (Agilent Technologies) and used in dual colour microarray hybridization with the Agilent *Arabidopsis* v4 oligo microarray slide. A dye-swap experiment was performed with two different RNA populations to eliminate the signal variation caused by the differential labelling efficiency of Cy3 and Cy5 dyes. The microarray data were normalized by the LOWESS method using the Feature Extraction software v. 10.7 (Agilent Technologies) and the expression ratios were analysed (Non-Uniformity Outlier and Feature Population Outlier). Data with a *P*-value of >0.01 were eliminated. The genes that showed a consistent expression pattern in *cas-1* and at least a twofold difference in the expression level in both slides are listed in Supplementary Data 1.

The genes induced by flg22 (ref. 17), by illumination of the *flu* mutant (chloroplast-derived ¹O₂)²⁹ and the *flu* mutant overexpressing thylakoid-localized ascorbate peroxidase²⁹ and by MV³⁰ were obtained from publications. To extract *flu*-regulated genes, raw signal intensity data (GSE10812) were obtained from the NCBI GEO database²⁹. The genes that revealed a consistent expression pattern at 2 h after a dark-to-light shift in the *flu* mutant compared with wild type and exhibited at least a threefold difference in the expression level were used for this analysis.

Gene ontology and promoter sequence analyses. Gene ontology analysis was performed with the Arabidopsis Classification SuperViewer at the BAR of the University of Toronto. We compared the gene expression profiles of our microarray experiments with available expression data via the expression browser at BAR. We also searched for over-represented *cis*-elements in the 500-bp upstream regions of the down- and upregulated genes in flg22-treated *cas-1* plants using the Regulatory Sequence Analysis tool (RSAT; <http://rsat.ulb.ac.be/rsat>).

References

1. Tsuda, K. & Katagiri, F. Comparing signaling mechanisms engaged in pattern-triggered and effector-triggered immunity. *Curr. Opin. Plant Biol.* **13**, 459–465 (2010).
2. Grant, M. R. & Jones, J. D. Hormone (dis)harmony moulds plant health and disease. *Science* **324**, 750–752 (2009).
3. Padmanabhan, M. S. & Dinesh-Kumar, S. P. All hands on deck—the role of chloroplasts, endoplasmic reticulum, and the nucleus in driving plant innate immunity. *Mol. Plant Microbe Interact.* **23**, 1368–1380 (2010).
4. McAinsh, M. R. & Pittman, J. K. Shaping the calcium signature. *New Phytol.* **181**, 275–294 (2009).
5. Costa, A. *et al.* H₂O₂ in plant peroxisomes: an *in vivo* analysis uncovers a Ca²⁺-dependent scavenging system. *Plant J.* **62**, 760–772 (2010).
6. Pinton, P., Giorgi, C., Siviero, R., Zecchini, E. & Rizzuto, R. Calcium and apoptosis: ER-mitochondria Ca²⁺ transfer in the control of apoptosis. *Oncogene* **27**, 6407–6418 (2008).
7. Han, S., Tang, R., Anderson, L. K., Woerner, T. E. & Pei, Z.-M. A cell surface receptor mediates extracellular Ca²⁺ sensing in guard cells. *Nature* **425**, 196–200 (2003).
8. Nomura, H., Komori, T., Kobori, M., Nakahira, Y. & Shiina, T. Evidence for chloroplast control of external Ca²⁺-induced cytosolic Ca²⁺ transients and stomatal closure. *Plant J.* **53**, 988–998 (2008).
9. Weinel, S. *et al.* A plastid protein crucial for Ca²⁺-regulated stomatal responses. *New Phytol.* **179**, 675–686 (2008).
10. Vainonen, J. P. *et al.* Light regulation of CaS, a novel phosphoprotein in the thylakoid membrane of *Arabidopsis thaliana*. *FEBS J.* **275**, 1767–1777 (2008).
11. Sai, J. & Johnson, C. H. Dark-stimulated calcium ion fluxes in the chloroplast stroma and cytosol. *Plant Cell* **14**, 1279–1291 (2002).
12. Petroustos, D. *et al.* The chloroplast calcium sensor CAS is required for photo-acclimation in *Chlamydomonas reinhardtii*. *Plant Cell* **23**, 2950–2963 (2011).
13. Strawn, M. A. *et al.* *Arabidopsis* isochorismate synthase functional in pathogen-induced salicylate biosynthesis exhibits properties consistent with a role in diverse stress responses. *J. Biol. Chem.* **282**, 5919–5933 (2007).
14. Tsuda, K., Sato, M., Glazebrook, J., Cohen, J. D. & Katagiri, F. Interplay between MAMP-triggered and SA-mediated defense responses. *Plant J.* **53**, 763–775 (2008).
15. Thilmony, R., Underwood, W. & He, S. Y. Genome-wide transcriptional analysis of the *Arabidopsis thaliana* interaction with the plant pathogen *Pseudomonas syringae* pv. *tomato* DC3000 and the human pathogen *Escherichia coli* O157:H7. *Plant J.* **46**, 34–53 (2006).
16. Zipfel, C. Pattern-recognition receptors in plant innate immunity. *Curr. Opin. Immunol.* **20**, 10–16 (2008).
17. Denoux, C. *et al.* Activation of defense response pathways by OGs and Flg22 elicitors in *Arabidopsis* seedlings. *Mol. Plant* **1**, 423–445 (2009).
18. Toufighi, K., Brady, S. M., Austin, R., Ly, E. & Provart, N. J. The botany array resource: e-Northers, expression angling, and promoter analyses. *Plant J.* **43**, 153–163 (2005).
19. Rushton, P. J., Somssich, I. E., Ringler, P. & Shen, Q. J. WRKY transcription factors. *Trend. Plant Sci.* **15**, 247–258 (2010).
20. Ishihama, N., Yamada, R., Yoshioka, M., Katou, S. & Yoshioka, H. Phosphorylation of the *Nicotiana benthamiana* WRKY8 transcription factor by MAPK functions in the defense response. *Plant Cell* **23**, 1153–1170 (2011).
21. van Verk, M. C., Bol, J. F. & Linthorst, H. J. WRKY transcription factors involved in activation of SA biosynthesis genes. *BMC Plant Biol.* **11**, 89 (2011).
22. Zhang, Y. *et al.* Control of salicylic acid synthesis and systemic acquired resistance by two members of a plant-specific family of transcription factors. *Proc. Natl Acad. Sci. USA* **107**, 18220–18225 (2010).
23. Waters, M. T. *et al.* GLK transcription factors coordinate expression of the photosynthetic apparatus in *Arabidopsis*. *Plant Cell* **21**, 1109–1128 (2009).
24. Sun, C.-W., Huang, Y.-C. & Chang, H.-Y. CIA2 coordinately up-regulates protein import and synthesis in leaf chloroplasts. *Plant Physiol.* **150**, 879–888 (2009).
25. Hudson, D. *et al.* *GNC* and *CGA1* modulate chlorophyll biosynthesis and glutamate synthase (*GLU1/Fd-GOGAT*) expression in *Arabidopsis*. *PLoS One* **6**, e26765 (2011).
26. Shiina, T., Tsunoyama, Y., Nakahira, Y. & Khan, M. S. Plastid RNA polymerases, promoters, and transcription regulators in higher plants. *Int. Rev. Cytol.* **244**, 1–68 (2005).
27. Maclean, D., Jerome, C. A., Brown, A. P. C. & Gray, J. C. Co-regulation of nuclear genes encoding plastid ribosomal proteins by light and plastid signals during seedling development in tobacco and *Arabidopsis*. *Plant Mol. Biol.* **66**, 475–490 (2008).
28. Woodson, J. D. & Chory, J. Coordination of gene expression between organellar and nuclear genomes. *Nat. Rev. Genet.* **9**, 383–395 (2008).
29. Laloi, C. *et al.* Cross-talk between singlet oxygen- and hydrogen peroxide-dependent signaling of stress responses in *Arabidopsis thaliana*. *Proc. Natl. Acad. Sci. USA* **104**, 672–677 (2007).
30. Scarpeci, T. E., Zanon, M. I., Carrillo, N., Mueller-Roeber, B. & Valle, E. M. Generation of superoxide anion in chloroplasts of *Arabidopsis thaliana* during active photosynthesis: a focus on rapidly induced genes. *Plant Mol. Biol.* **66**, 361–378 (2008).
31. Bolton, M. D. Primary metabolism and plant defense-fuel for the fire. *Mol. Plant Microbe Interact.* **22**, 487–497 (2009).
32. Tosti, N. *et al.* Gene expression profiles of O₃-treated *Arabidopsis* plants. *Plant Cell Environ.* **29**, 1686–1702 (2006).
33. Fernández, A. P. & Strand, A. Retrograde signaling and plant stress: plastid signals initiate cellular stress responses. *Curr. Opin. Plant Biol.* **11**, 509–513 (2008).
34. Zurbriggen, M. D. *et al.* Chloroplast-generated reactive oxygen species play a major role in localized cell death during the non-host interaction between tobacco and *Xanthomonas campestris* pv. *vesicatoria*. *Plant J.* **60**, 962–973 (2009).

35. Wang, W.-H. *et al.* Calcium-sensing receptor regulates stomatal closure through hydrogen peroxide and nitric oxide in response to extracellular calcium in *Arabidopsis*. *J. Exp. Bot.* **63**, 177–190 (2012).
36. Lee, K. P., Kim, C., Landgraf, F. & Apel, K. EXECUTER1- and EXECUTER2-dependent transfer of stress-related signals from the plastid to the nucleus of *Arabidopsis thaliana*. *Proc. Natl Acad. Sci. USA* **104**, 10270–10275 (2007).
37. Oschsenbein, C. *et al.* The role of *EDS1* (enhanced disease susceptibility) during singlet oxygen-mediated stress responses of *Arabidopsis*. *Plant J.* **47**, 445–456 (2006).
38. Xu, X., Hu, X., Neill, S. J., Fang, J. & Cai, W. Fungal elicitor induces singlet oxygen generation, ethylene release and saponin synthesis in cultured cells of *Panax ginseng* C. A. Meyer. *Plant Cell Physiol.* **46**, 947–954 (2005).
39. Saibo, N. J., Lourenço, T. & Oliveira, M. M. Transcription factors and regulation of photosynthetic and related metabolism under environmental stresses. *Ann. Bot.* **103**, 609–623 (2009).
40. Kallenbach, M., Alagna, F., Baldwin, I. T. & Bonaventure, G. *Nicotiana attenuata* SIPK, WIPK, NPR1 and fatty acid-amino acid conjugates participate in the induction of JA biosynthesis by affecting early enzymatic steps in the pathway. *Plant Physiol.* **152**, 96–106 (2010).
41. Tozawa, Y. *et al.* Calcium-activated (p)ppGpp synthetase in chloroplasts of land plants. *J. Biol. Chem.* **282**, 35536–35545 (2007).
42. Kreimer, G., Melkonian, M., Holtum, J. A. M. & Latzko, E. Stromal free calcium concentration and light-mediated activation of chloroplast fructose-1,6-bisphosphatase. *Plant Physiol.* **86**, 423–428 (1998).
43. Caporaletti, D. *et al.* Non-reductive modulation of chloroplast fructose-1,6-bisphosphatase by 2-Cys peroxiredoxin. *Biochem. Biophys. Res. Commun.* **355**, 722–727 (2007).
44. Miqyas, M., van Gorkom, H. J. & Yocum, C. F. The PSII calcium site revisited. *Photosynth. Res.* **93**, 89–100 (2007).
45. Garmier, M. *et al.* Light and oxygen are not required for harpin-induced cell death. *J. Biol. Chem.* **282**, 37556–37566 (2007).
46. Boccara, M. *et al.* Early chloroplastic alterations analysed by optical coherence tomography during a harpin-induced hypersensitive response. *Plant J.* **50**, 338–346 (2007).
47. Triantaphylidès, C. & Havaux, M. Singlet oxygen in plants: production, detoxification and signaling. *Trends Plant Sci.* **14**, 219–228 (2009).
48. Jahns, P. & Holzwarth, A. R. The role of the xanthophyll cycle and of lutein in photoprotection of photosystem II. *Biochim. Biophys. Acta* **1817**, 182–193 (2012).
49. Roden, L. C. & Ingle, R. A. Lights, rhythms, infection: the role of light and the circadian clock in determining the outcome of plant-pathogen interactions. *Plant Cell* **21**, 2546–2552 (2009).
50. Wang, W. *et al.* Timing of plant immune responses by a central circadian regulator. *Nature* **470**, 110–114 (2011).
51. Huner, N. P. A., Öquist, G. & Sarhan, F. Energy balance and acclimation to light and cold. *Trends Plant Sci.* **3**, 224–230 (1998).
52. Tang, R.-H. *et al.* Coupling diurnal cytosolic Ca²⁺ oscillations to the CAS-IP₃ pathway in *Arabidopsis*. *Science* **315**, 1423–1426 (2007).
53. Knight, H., Trethewey, A. J. & Knight, M. R. Cold calcium signaling in *Arabidopsis* involves two cellular pools and a change in calcium signature after acclimation. *Plant Cell* **8**, 489–503 (1996).
54. Rodoriguez-Kabana, R., Godoy, G., Morgan-Jones, G. & Shelby, R. A. The determination of soil chitinase activity: conditions for assay and ecological studies. *Plant Soil* **75**, 95–106 (1983).
55. Kim, M. G. *et al.* Two *Pseudomonas syringae* Type III effectors inhibit RIN4-regulated basal defense in *Arabidopsis*. *Cell* **121**, 749–759 (2005).
56. Izumi, Y., Okazawa, A., Bamba, T., Kobayashi, A. & Fukusaki, E. Development of a method for comprehensive and quantitative analysis of plant hormones by highly sensitive nanoflow liquid chromatography–electrospray ionization–ion trap mass spectrometry. *Anal. Chim. Acta* **648**, 215–225 (1999).
57. Sugimoto, T. *et al.* Use of ultra-performance liquid chromatography/time-of-flight mass spectrometry with nozzle-skimmer fragmentation for comprehensive quantitative analysis of secondary metabolites in *Arabidopsis thaliana*. *J. Sep. Sci.* **34**, 3587–3596 (2011).
58. Ratcliff, F., Martin-Hernandez, A. M. & Baulcombe, D. C. Tobacco rattle virus as a vector for analysis of gene function by silencing. *Plant J.* **25**, 237–245 (2001).

Acknowledgements

We thank M. Isobe and M. Kuse for providing coelenterazine, D.C. Baulcombe for pTV00 vector, Y. Ohashi and I. Mitsuhashi for the *NtMEK2^{DD}* clone, P. Mullineaux and R. Hellens for pGreen binary vector, S. Kamoun for *INF1*, J.D.G. Jones for *cf9/Avr9* and the Leaf Tobacco Research Center, Japan Tobacco, for *N. benthamiana* seeds. We also thank Y. Kubo, M.H. Sato, Y. Yagi and Y. Ishizaki for discussions, and T. Kimura and K. Yamasaki for technical assistance. This work was supported by Grants-in-Aid (No. 20200060 to Y.N. and 22370022 to T.S.), Private University Strategic Research Foundation Support Program (S0801060) and Joint Research Program implemented at the Institute of Plant Science and Resources, Okayama University from MEXT, and this work was also supported by the Program for Promotion of Basic Research Activities for Innovative Biosciences (PROBRAIN).

Author contributions

H.N., H.Y. and T. Shiina designed the research plan; H.N., T.K., S.U., Y.K., K.S., K.N., T.F., S.S., I.N.S., H.Y., N.Y. and T. Shiina performed experiments; K.T., T. Sugimoto and E.F. carried out metabolome and hormone analyses; H.N. and T. Shiina wrote the manuscript.

Additional information

Accession codes: The *NbCAS* sequence has been deposited in the DNA Data Bank of Japan under accession code AB720027.

Supplementary Information accompanies this paper at <http://www.nature.com/naturecommunications>

Competing financial interests: The authors declare no competing financial interests.

Reprints and permission information is available online at <http://npg.nature.com/reprintsandpermissions/>

How to cite this article: Nomura, H. *et al.* Chloroplast-mediated activation of plant immunity signalling in *Arabidopsis*. *Nat. Commun.* 3:926 doi: 10.1038/ncomms1926 (2012).

Corrigendum: Chloroplast-mediated activation of plant immune signalling in *Arabidopsis*

Hironari Nomura, Teiko Komori, Shuhei Uemura, Yui Kanda, Koji Shimotani, Kana Nakai, Takuya Furuichi, Kohsuke Takebayashi, Takanori Sugimoto, Satoshi Sano, I Nengah Suwastika, Eiichiro Fukusaki, Hirofumi Yoshioka, Yoichi Nakahira & Takashi Shiina

Nature Communications 3:926 doi: 10.1038/ncomms1926 (2012); Published 26 Jun 2012; Updated 5 Feb 2013

The affiliation details for Hirofumi Yoshioka and Yoichi Nakahira are incorrect in this Article. The correct affiliations for these authors are listed below.

Hirofumi Yoshioka², Yoichi Nakahira^{1,5}

¹Graduate School of Life and Environmental Sciences, Kyoto Prefectural University, Sakyo-ku, Kyoto 606-8522, Japan. ²Graduate School of Bioagricultural Sciences, Nagoya University, Chikusa-ku, Nagoya 464-8601, Japan. ⁵The Venture Business Laboratory, Ehime University, Bunkyo-cho, Matsuyama 790-8577, Japan